

Baryon-Dark matter interaction in presence of magnetic fields in light of EDGES signal

Jitesh R. Bhatt,^{1,*} Pravin Kumar Natwariya^{1,2,†}, Alekha C. Nayak^{1,‡} and Arun Kumar Pandey^{1,§}

¹Physical Research Laboratory, Theoretical Physics Division, Ahmedabad 380 009, India

²Department of Physics, Indian Institute of Technology, Gandhinagar, Ahmedabad 382 424, India

(Dated: June 3, 2019)

Abstract: The Experiment to Detect the Global Epoch of reionization Signature (EDGES) collaboration has reported an excess absorption dip in the 21 cm signal during cosmic dawn era. The stronger than expected 21 absorption signal indicates that gas was much cooler than the standard cosmological prediction. The observed 21-cm signal can be explained by decreasing the gas temperature via baryon-DM interaction. In this work, we study the temperature evolution of the gas and Dark Matter (DM) in the presence of magnetic fields. The magnetic heating via ambipolar diffusion and the turbulent decay increases both the gas and DM temperature at low redshift and this heating is more in the favour of baryons compared to DM. In the presence of strong magnetic field, a large baryon-DM interaction cross section is required to balance magnetic heating to explain the EDGES signal as compared to weak magnetic field. We also study the brightness temperature during the cosmic dawn era and put constraint on the strength of the magnetic field for a particular mass and baryon-DM cross section.

Keywords: Magnetic fields, 21-cm signal, Baryon-dark matter interaction, EDGES signal

I. INTRODUCTION

Within the standard cold dark matter cosmology (Λ CDM), free electrons and protons cool sufficiently after 3×10^5 years of big-bang to form neutral hydrogen atoms. At the end of recombination ($z \approx 1100$), matter decouples from the cosmic microwave background (CMB) photons and the temperature reaches around 3000 K. After that, the dark age begins and the Universe becomes homogenous. Later during the cosmic dawn era ($15 < z < 35$), over density grow in the matter perturbations and collapse to form the first star and galaxy in the Universe. During the dark ages, residual electrons from the recombination scatter off the baryons to maintain the thermal equilibrium until $z \approx 200$. Subsequently, gas cools adiabatically due to the thermal expansion of the Universe and the gas temperature reaches to ≈ 6.8 K at $z = 17$.

During the cosmic dawn era, the gas temperature is lower than the CMB temperature hence hyperfine transitions in the neutral hydrogen atoms produce 21-cm absorption spectra. The hyperfine transitions are due to the CMB photons, gas collisions and the Ly- α radiations from the first star. 21-cm absorption line leaves an imprint of spectral distortion in the low-frequency tail of the CMB spectrum. The observation of the 21-cm line can give logical reason behind the density fluctuations [1], cosmic reionization [2] and X-ray heating of the IGM [3]. Recently, ‘‘Experiment to Detect the Global Epoch of Reionization Signature (EDGES)’’ collaboration reported the first detection of such absorption signal centred at 78 MHz [4]. The observed absorption dip at $z \approx 17$ is approximately 2.5 times larger than the standard Λ CDM model prediction [4]. Several attempts have been made in the literature to explain the observed EDGES absorption dip. One possible scenario to explain the observed spectrum is to cool the gas in

the Inter-Galactic Medium (IGM) below the standard Λ CDM prediction. Since the DM in the Λ CDM model is colder than the gas, elastic scattering of baryon with DM can cool the gas [5, 6]. A non-standard Coulomb interaction between baryon with dark matter: $\sigma = \hat{\sigma}v^{-4}$ has been considered to explain the EDGES signal, where v is the relative velocity between the dark matter and the baryons [5, 7, 8]. Millicharge dark matter particle has been proposed to cool the gas temperature via DM-baryon interaction [4, 6]. Substantial part of the DM mass and coupling are tightly constrained by the cosmological and the astrophysical observations [5, 6, 9, 10]. Increasing the background radio photons during the cosmic dawn era and modifying the cosmological evolutions are the other possible explanations of the EDGES signal [11]. In Ref. [12–14], authors have studied the DM annihilation/decay which can inject the energy and heats the gas. They have also constrained the annihilation/decay rate of DM such that it can not erase the standard 21 cm signal. In Ref. [15], authors have considered the dark matter viscosity to heat the gas and dark matter in the context of the observed 21 cm signal. Another possible process to heat the gas is, to consider a decaying magneto-hydrodynamics, where a decaying magnetic field can heat the IGM. In the present work, we study the effect of magnetic heating on the temperature evolution of the gas, DM and the brightness temperature in presence of the baryon-dark matter interaction during the cosmic dawn era.

These magnetic fields could have generated during the structure formation or in the early Universe [16–20]. It is observed that the magnetic fields are present on all length scales (i.e. at the scales of galaxies and the clusters). They have a strength of the order of few μ G at a coherent length scale of a few tens of kpc for clusters of galaxies and a few kpc for galaxies [21, 22]. The strength of these magnetic fields is constrained from the structure formation, big bang nucleosynthesis (BBN) and temperature anisotropies and polarization of cosmic microwave background (CMB) [23, 24]. Anisotropy generated by homogeneous magnetic fields, whose maximal amplitude measured by PLANCK today is $B_0 \leq 4.4$ nG at a

* jeet@prl.res.in

† pravin@prl.res.in

‡ alekha@prl.res.in

§ arunp77@gmail.com

comoving scale of 1 Mpc [25]. From the data of Fermi and High Energy Stereoscopic System (HESS) gamma-ray telescopes, the peak strength of the magnetic field at a length scale of 1 Mpc is of the order of few nG [22]. However, the upper bound on the amplitude of the magnetic field, obtained from BBN is $\sim 10^{-6}$ G at a comoving length scale of ~ 100 pc [26, 27]. If strong magnetic fields were present at the time of nucleosynthesis, the abundance of relic ${}^4\text{He}$ and other light elements could have different values than we observe today [28, 29]. Therefore, to satisfy the current observational limits on the light element abundances, the strength of these magnetic fields should have a value of the order of $\approx 10^{-7}$ G, at the present time [30, 31]. It has also been shown that, in the presence of the magnetic fields, thermal evolution of the baryon, after recombination could be modified, as these magnetic fields may decay and heats the IGM. This decay occurs through standard ambipolar diffusion and forward cascade of the magnetic energy [31]. Therefore reionization of IGM and structure formation is connected to the thermal evolution of the baryons and decoupling of the photons at recombination.

The present work is divided into the following sections: in section (II), we have revisited the 21-cm observed signal from the EDGES; in section (III), a brief description of the Primordial magnetic fields (PMF) and it's decay is discussed; section (IV) contains the result obtained and a detailed discussion. In the end, we have summarized and concluded our work in section (VI).

II. 21 CM SIGNAL AND EDGES OBSERVATION

At the end of recombination, the baryon number density of the Universe mostly dominated by the neutral hydrogen, small fraction of helium, residual free electrons and protons. The hyperfine interaction between spin of the electron and proton split the ground state of neutral hydrogen atom into singlet and triplet states with an energy difference of $E_{21} = 5.9 \times 10^{-6}$ eV $= 2\pi/(21 \text{ cm})$. Relative number densities of neutral hydrogen in the singlet and triplet state, define the spin temperature (T_S) of the gas, and is given by the following relation:

$$\frac{n_1}{n_0} = \frac{g_1}{g_0} e^{-\frac{E_{21}}{T_S}} \approx 3 \left(1 - \frac{E_{21}}{T_S}\right), \quad (1)$$

here n_0 and n_1 are the number densities in the singlet and triplet states respectively. Three competing mechanisms that determine the spin temperature are: gas collision, emission/absorption of CMB photon and Ly- α radiation from the first star. Equilibrium balance between singlet and triplet state due to these effects set the spin temperature [32]

$$T_S^{-1} = \frac{T_{\text{CMB}}^{-1} + x_c T_{\text{gas}}^{-1} + x_\alpha T_{\text{Ly}\alpha}^{-1}}{1 + x_c + x_\alpha}, \quad (2)$$

where T_{CMB} , T_{gas} and $T_{\text{Ly}\alpha}$ are the CMB, kinetic and the Ly α temperature of the gas respectively. x_c and x_α are the collisional and Ly α coupling respectively,

$$x_c = \frac{E_{21}}{T_{\text{gas}}} \frac{C_{10}}{A_{10}}, \quad x_\alpha = \frac{T_S}{T_{\text{Ly}\alpha}} \frac{P_{01}^w}{A_{10}},$$

where C_{10} is the collision rate between $H-H$, $H-e$, $p-H$ and P_{01}^w is the excitation rate due to Ly- α radiation and $A_{10} = 2.9 \times 10^{-15} \text{sec}^{-1}$ is the Einstein coefficient for spontaneous emission. After the first star formation, a large number of Ly α photons scattered with the gas, and brought the radiation and the gas into a local thermal equilibrium [32]. Hence during the cosmic dawn era $T_{\text{gas}} \approx T_\alpha$. The 21 cm signal can be described, in terms of the redshifted differential brightness temperature [32]

$$T_{21} = \frac{1}{1+z} (T_S - T_{\text{CMB}})(1 - \exp^{-\tau}), \quad (3)$$

where optical depth $\tau = \frac{3\lambda_{21}^2 A_{10} n_H}{16 T_S H(z)}$, n_H is the hydrogen number density and $H(z)$ is the Hubble rate. Depending on the spin and the CMB temperature, three scenarios arise: (i) when $T_S = T_{\text{CMB}}$, then no signal is observed; (ii) if $T_S < T_{\text{CMB}}$, photon get absorbed by the gas and absorption spectra is observed; and (iii) if $T_S > T_{\text{CMB}}$, then it leaves an imprint of emission spectra.

Evolution of the 21 cm signal is as follows: after recombination at $z \sim 1100$ down to $z \sim 200$, the residual free electrons undergo Compton scattering to maintain thermal equilibrium between the gas and CMB, and collisions among the gas is dominant, i.e. $x_c \gg 1$, x_α [5, 32], which set $T_S = T_{\text{CMB}}$. Hence, 21 cm signal is not observed during this era. Below $z \sim 200$ until $z \sim 40$, the gas cools adiabatically and it falls below CMB temperature, which implies the early 21 cm absorption signal. The strength of this absorption signal is too small to observe. Below $z \sim 40$ down to the first star formation, gas cools sufficiently due to the expansion and the collisional coupling becomes very small due to the dilution, i.e. $x_c, x_\alpha \rightarrow 0$ [5, 32]. This implies, $T_S = T_{\text{CMB}}$, hence no 21 cm signal during this period. After the first star formation, a transition between the singlet and triplet states occurs due to the Ly α photons emitted from the first stars via Wouthuysen-Field (WF) effect [33, 34]. Ly α photons couple the spin temperature to the gas temperature. In this era, $x_\alpha \gg 1$, hence spin temperature and the gas temperature become equal to each other i.e., $T_S = T_{\text{gas}} < T_{\text{CMB}}$. Thus an imprint of the 21-cm absorption signal can be seen at the low-frequency tail of the CMB spectrum. Below $z \sim 15$ until $z \sim 7$, X-ray from the active galactic nuclei heats the gas above the CMB temperature and we observe an emission signal [32]. Below $z \sim 7$ neutral hydrogen became ionized and the signal disappears.

Recently, the EDGES collaboration reported the global brightness temperature at $z = 17$

$$T_{21}^{\text{obs}}(z = 17) = -500_{-300}^{+200} \text{ mK}, \quad (4)$$

and corresponding gas temperature is $3.26_{-1.58}^{+1.94}$ K [4]. On the contrary, standard ΛCDM predicts the gas temperature 6.8 K at $z = 17$ and corresponding brightness temperature $T_{21} \geq -220$ mK [5]. In order to explain the EDGES absorption signal, the gas temperature needs to be cooler than the ΛCDM prediction. During the Cosmic dawn era, the Universe was at its coldest phase, and the relative velocity between the DM and baryon was very small [$\mathcal{O}(10^{-6})$]. Also, the temperature of the dark matter is colder than the baryon temperature

during this period, so an interaction of the baryon with dark matter can cool the gas temperature. Since the relative velocity is small, scattering cross section of the type $\sigma = \hat{\sigma}v^{-4}$ can enhance the interaction rate and cool the gas sufficiently to explain EDGES absorption dip [7, 8]. In this work, we consider magnetic heating of the gas and the DM via ambipolar and turbulent decay to study the EDGES 21 cm signal.

III. PRIMORDIAL MAGNETIC FIELDS AFTER THE RECOMBINATION ERA

In this section, we present the effect of PMFs on the thermal history of the Universe. We assume that, due to some early Universe process, tangled magnetic fields were present at a sufficiently large length scale after the recombination era. We also consider a very small velocity induced by the PMFs to avoid any dissipations of the initial magnetic fields due to viscosity and other dissipation [35, 36]. This is applicable in linear regime and magnetic fields evolve adiabatically as $\mathbf{B}(t, \mathbf{x}) = \tilde{\mathbf{B}}(\mathbf{x})/a(t)^2$, where \mathbf{x} is the comoving coordinate, $\tilde{\mathbf{B}}$ is the comoving strength of the magnetic fields and $a(t)$ is the scale factor. Since plasma in the early Universe remains highly conductive, the adiabatic evolution of the magnetic fields is true. However, at a sufficiently small scale, when non-linear effects operate, adiabatic decay no longer satisfy. In this case, it is needed to consider Euler Eqs. along with the magnetic induction equation and Maxwell's Eqs. to understand the dynamics of the fluid.

In the present work, we consider an isotropic and homogeneous Gaussian random magnetic field, whose power spectrum is given by the following equation

$$\langle \tilde{\mathbf{B}}_i(\mathbf{k}) \tilde{\mathbf{B}}_j^*(\mathbf{q}) \rangle = \frac{(2\pi)^3}{2} \delta_D^3(\mathbf{k} - \mathbf{q}) \left(\delta_{ij} - \frac{k_i k_j}{k^2} \right) \mathcal{P}_B(k), \quad (5)$$

where $\mathcal{P}_B(k)$ is the magnetic power spectrum and $k = |\mathbf{k}|$ is the comoving wave number. For simplicity, we consider a power law spectrum of the magnetic fields $\mathcal{P}_B(k) = A k^{n_B}$ for $k < k_{\max}$ (k_{\max} is calculated by the damping at recombination due to the viscosity) [35, 36]. Here n_B and A are spectral index and the normalization constants respectively. In particular, $n_B = 2$ for white noise [37], $n_B = 4$ for Batchelor spectrum [38] and $n_B = -2.9$ for nearly scale invariant spectrum [31]. The amplitude (A) can be obtained by demanding the magnetic fields are smooth over the cut off scale, and after that $\mathcal{P}_B(k) = 0$. Once the recombination period end, baryons and CMB photons decouple and their velocity start to increase. Eventually, these particles achieve a common velocity, determined by the equipartition between the magnetic field and kinetic energy of the baryon gas. This velocity is given by the Alfvén velocity $v_A = c B_0 / \sqrt{4\pi\rho_{b_0} a(t)}$, here ρ_{b_0} is the present baryon density and B_0 is the currently observed strength of the magnetic field at Mpc scale. The cut off scale is defined as $k_{\max} \approx 2\pi \frac{H_0}{v_A}$. Therefore, the cut off value from this relation can be written

as [31, 39]:

$$\frac{k_{\max}}{2\pi \text{Mpc}^{-1}} = \left[1.32 \times 10^{-3} \left(\frac{B_0}{\text{InG}} \right)^2 \left(\frac{\Omega_b h^2}{0.02} \right)^{-1} \left(\frac{\Omega_m h^2}{0.15} \right) \right]^{\frac{-1}{(n_B+5)}}, \quad (6)$$

here Ω_b , Ω_m , and h are the cosmological parameters and have the mathematical value $h = 0.674$ ($H_0 = h \times 100 \text{ km-s}^{-1} \text{ Mpc}$), $h^2 \Omega_b = 0.0224 \pm 0.0001$, $h^2 \Omega_m = 0.143$ [40].

Dissipation of magnetic energy

After recombination, any present magnetic field dissipates its energy and heats the gas through two mechanisms, namely the ambipolar diffusion and the turbulent decay [31, 39]. The heating of the gas gives a considerable change in the thermal evolution of neutral atoms. The velocity difference in the ionized and neutral particles after the recombination leads to the ambipolar diffusion of the magnetic energy. Direct cascade happens due to the non-linear processes, which couples the different modes and the cascading of magnetic energy from large to small scale. This happens through the breaking of the larger eddy into the smaller eddies, when eddy turn over time t_{eddy} is equal to the Hubble time i.e. ($t_{\text{eddy}} \sim H^{-1}$). The energy dissipation due to ambipolar and direct cascade can be given by [41, 42],

$$\Gamma_{\text{ambi}} = \frac{\rho_n}{16\pi^2 \gamma \rho_b^2 \rho_i} |\nabla \times \mathbf{B} \times \mathbf{B}|^2, \quad (7)$$

$$\Gamma_{\text{decay}} = \frac{B_0^2(t)}{8\pi} \frac{3m}{2} \frac{[\ln(1 + t_{\text{eddy}}/t_i)]^m H(t)}{[\ln(1 + t_{\text{eddy}}/t_i) + \ln(t/t_i)]^{m+1}}, \quad (8)$$

where ρ_n and ρ_i are the mass densities of neutral and the ionized atoms respectively, t is the cosmological time at a generic red shift z , t_{eddy} is the physical decay time scale for the turbulent and t_i is In Eq. (8), initial time at which decay starts. $m = 2(n_B + 3)/(n_B + 5)$. For the present scenario γ is given by [42–45],

$$\gamma = \frac{\frac{1}{2} n_H \langle \sigma v \rangle_{\text{H}^+, \text{H}} + \frac{4}{3} n_{\text{He}} \langle \sigma v \rangle_{\text{H}^+, \text{He}}}{m_H [n_H + 4n_{\text{He}}]}, \quad (9)$$

where m_H is the mass of the hydrogen and n_{He} is the number density of the helium atom. The absolute values of the Lorentz force and magnetic energy in Eqs. (7) and (8) can be obtained by considering a suitable power law spectrum of the magnetic field. This can be done using following correlation integrals: $|\nabla \times \mathbf{B} \times \mathbf{B}|^2 = \int (dk/2\pi)^3 \int (dq/2\pi)^3 k^2 \mathcal{P}_B(t, k) \mathcal{P}_B(t, q) (1+z)^{10}$ and $|\mathbf{B}|^2 = \int (dk/2\pi)^3 \mathcal{P}_B(t, k) (1+z)^4$. However, in the present work, we have taken approximate value of the ambipolar diffusion term, which is [46]

$$\Gamma_{\text{ambi}} \sim \frac{\rho_n}{16\pi^2 \gamma \rho_b^2 \rho_i} \frac{B^4}{L^2}, \quad (10)$$

here L is a typical length scale. To sum up, the time evolution of the magnetic energy can be written as [31, 36]

$$\frac{d}{dt} \left(\frac{|\mathbf{B}|^2}{8\pi} \right) = -4H(t) \left(\frac{|\mathbf{B}|^2}{8\pi} \right) - \Gamma_{\text{ambi}} - \Gamma_{\text{decay}}. \quad (11)$$

IV. BARYON AND DARK MATTER INTERACTION IN PRESENCE OF MAGNETIC FIELD

In this section, we discuss the effects of magnetic field on the baryon and DM temperature when they are interacting with each other. Temperature evolutions of the DM and baryon, having relative velocity, in the presence of the magnetic field are given below

$$\frac{dT_{\text{gas}}}{dz} = \frac{2T_{\text{gas}}}{(1+z)} + \frac{\Gamma_C}{(1+z)H}(T_{\text{gas}} - T_{\text{CMB}}) + \frac{2}{3(1+z)H} \frac{dQ_{\text{gas}}}{dt} - \frac{2\Gamma_{\text{heat}}}{3(1+z)H}, \quad (12)$$

$$\frac{dT_d}{dz} = \frac{2T_d}{(1+z)} + \frac{2}{3(1+z)H} \frac{dQ_d}{dt} \quad (13)$$

$$\frac{dv}{dz} = \frac{v}{(1+z)} + \frac{D(v)}{(1+z)H} \quad (14)$$

where T_d and m_d are temperature and mass of the DM respectively, H is the Hubble expansion rate and Γ_C is the Compton scattering rate, defined as

$$\Gamma_C = \frac{8\sigma_T a_r T_{\text{CMB}}^4 x_e}{2(1+x_e+x_{\text{He}})m_e}.$$

where $x_e = n_e/n_H$ is the electron fraction, x_{He} is the helium fraction, a_r is the radiation constant and σ_T is the Thomson scattering cross section. Drag term $D(v)$ is given by

$$D(v) \equiv \frac{\rho_m \hat{\sigma}}{m_H + m_d} \frac{1}{v^2} F(r), \quad (15)$$

where ρ_M is matter density and

$$F(r) \equiv \text{erf}\left(\frac{r}{\sqrt{2}}\right) - \sqrt{\frac{2}{\pi}} r e^{-r^2/2},$$

with $r = \frac{v}{u_{\text{th}}}$ and $u_{\text{th}} = \sqrt{\frac{T_{\text{gas}}}{m_H} + \frac{T_d}{m_d}}$. Heat transfer of the gas per unit time is given by [47]

$$\frac{dQ_{\text{gas}}}{dt} = \frac{2m_H \rho_d \hat{\sigma} e^{-r^2/2}}{\sqrt{2\pi}(m_H + m_d)^2 u_{\text{th}}^3} (T_d - T_{\text{gas}}) + \frac{\mu \rho_d}{\rho_M} v D(v), \quad (16)$$

where μ is the reduced mass of DM and baryon, $\hat{\sigma}$ is DM-gas scattering cross-section. In Eq.(16), the first term represents the baryonic cooling due to its interaction with the DM and the second term represents the heating due to the drag term. The relative velocity between the dark matter and the gas, produce friction between two fluid which is responsible for the drag term. Heat transfer rate for dark matter, $\frac{dQ_d}{dt}$ can be obtained by interchanging $gas \leftrightarrow d$ in Eq. (16). Temperature evolution of the DM and gas require electron ionization fraction [48]:

$$\frac{dx_e}{dz} = \frac{1}{H(1+z)} \frac{\frac{3}{4}R_{\text{Ly}\alpha} + \frac{1}{4}\Lambda_{2s,1s}}{\beta_B + \frac{3}{4}R_{\text{Ly}\alpha} + \frac{1}{4}\Lambda_{2s,1s}} - \left(n_H x_e^2 \alpha_B - 4(1-x_e)\beta_B e^{-E_{21}/T_{\text{CMB}}}\right) \quad (17)$$

where β_B and α_B are the photoionization rate and case-B recombination coefficient respectively. E_{21} is energy of Ly α

wavelength photon and $\Lambda_{2s,1s} = 8.22 \text{ sec}^{-1}$ is the hydrogen two photon decay rate. The escape rate of Ly α is given by: $R_{\text{Ly}\alpha} = \frac{8\pi H}{3n_H(1-x_e)\lambda_{\text{Ly}\alpha}^3}$, $\lambda_{\text{Ly}\alpha}$ is the rest wavelength of Ly α photon. As it has been confirmed in Ref. [49], that cooling due to effects like Lyman- α emission, Bremsstrahlung and recombination does not have that much effects on the dynamics of the gas and DM, therefore, we have not considered these effects in our present work.

V. RESULTS AND DISCUSSION

Solving Eqs. (11)-(14) and Eq. (17) along with the Eq. (11) and setting initial condition $T_{\text{gas}}(1010) = 2749.92 \text{ K} = T_{\text{CMB}}(1010)$, $T_d(1010) = 0$, $x_e(1010) = 0.057$ and $B_0(1+z)^2$ initial magnetic field strength, we get the temperature evolution of the gas and DM for different DM mass, DM-baryon interaction cross-section and magnetic field. Figure (1) shows the evolution of the gas and DM temperature with redshift z and the solid blue line corresponds to gas temperature when both the magnetic field and DM-baryon interaction are zero. In this case, gas temperature falls as $T_{\text{gas}} \propto (1+z)^2$ and reaches 6.8 K at $z = 17$. In figure (1a), temperature evolution of the gas and the DM for different magnetic fields is given for different values of the magnetic field at constant $\hat{\sigma} = 10^{-41} \text{ cm}^2$ and $m_d = 0.1 \text{ GeV}$. For $B_0 = 10^{-5}$ (10^{-6}) G, gas temperature falls down due to Hubble expansion and interaction with dark matter till $z \approx 30$ ($z \approx 20$), then temperature rises due to magnetic heating term. For $B_0 = 10^{-5}$ G, the temperature of the DM also increases due to the coupling between the DM and baryons at lower redshift. Larger the strength of the magnetic field, earlier the heating begins, and heating of the gas is higher compared to the DM at low redshift. Although dark matter temperature at $z \sim 1010$ is taken to be zero, it heats up due to the drag term in Eq. (15) and heat transfer from hydrogen. At low redshift, temperature of dark matter for $B_0 = 10^{-5}$ G is larger compared to $B_0 = 10^{-6}$ G, because temperature of gas is higher for $B_0 = 10^{-5}$ G, its coupling with DM raises the DM temperature. Figure (1b) shows the temperature evolution of gas and DM for different DM-baryon interaction cross-section when magnetic field $B_0 = 10^{-6}$ G and DM mass $m_d = 0.1 \text{ GeV}$ are fixed. Larger the interaction between gas and DM, more heat transfers from gas to the DM and cools the gas efficiently. For $B_0 = 10^{-6}$ G and $\hat{\sigma} = 10^{-41} \text{ cm}^2$, temperature evolution for different dark matter mass is shown in Fig. (1c). As we increase the DM mass from 0.1 GeV to 1 GeV temperature of both the DM and gas increases, because the heating due to the drag term in (15) become more efficient for large dark matter mass [47]. This drag heating is important when mass of DM is comparable and greater than 1 GeV[47]. Below $z \sim 50$, in addition to heating due to the drag term, magnetic heating also contribute to the gas temperature, hence the gas temperature for $m_d = 1 \text{ GeV}$ is higher than $m_d = 0.1 \text{ GeV}$.

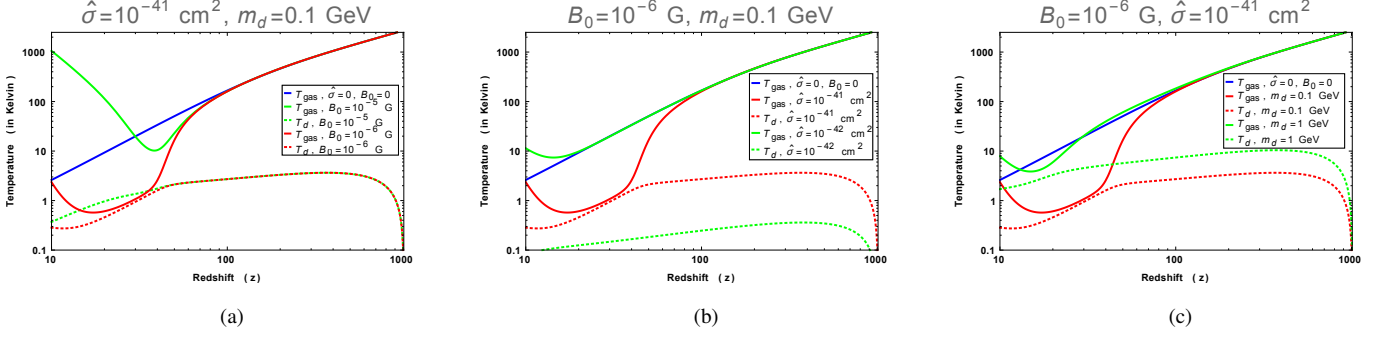


FIG. 1: Temperature evolution of baryon and DM in the presence of magnetic field and baryon-DM interaction. Blue line corresponds to temperature evolution of gas in the absence of both magnetic heating and baryon-DM interaction. The red (green) solid lines represents the variation of the gas temperature and the dotted red (green) line shows the variation of the DM temperature in presence of magnetic field and the baryon-DM interaction.

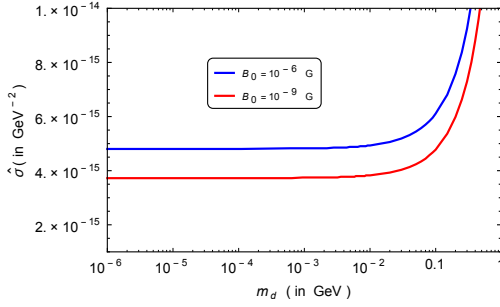


FIG. 2: DM-baryon cross section required for EDGES signal (i.e. $T_{\text{gas}} = 3.26\text{K}$) in the presence of magnetic field. The solid blue and red line correspond to $B_0 = 10^{-6}\text{G}$ and 10^{-9}G respectively. ($1\text{ GeV}^{-2} = 3.89 \times 10^{-28}\text{ cm}^2$)

Correlation between mass of DM and baryon-DM cross section from EDGES observation

As discussed above, in presence of a large magnetic field, temperature of the DM and gas increase during the cosmic dawn era, but the gas temperature increases more in comparison to the dark matter. Hence, the correlation between the mass of the dark matter and the baryon-DM interaction cross section for the EDGES signal changes for strong and weak magnetic fields. For $B_0 = 10^{-6}\text{G}$ and $B_0 = 10^{-9}\text{G}$, we solve Eqs.(11)-(17) for $T_{\text{gas}} = 3.26\text{K}$ at $z = 17$ to get m_d vs $\hat{\sigma}$ plot as shown in Fig.(2). As we increase the magnetic field from 10^{-6}G to 10^{-9}G , larger interaction cross section is required for $m_d \in \{10^{-6}, 0.1\}\text{ GeV}$ to maintain $T_{\text{gas}} = 3.26\text{K}$ at $z=17$. The heating effect due to large magnetic field is balanced by the large baryon-DM scattering cross section. When the DM mass approaches mass of hydrogen, the drag term in Eq.(15) also contribute to the heating of gas in addition to the magnetic heating. As discussed in [47], when $m_d \gg 1\text{ GeV}$, the drag term heat up both the fluid sufficiently such that we can not obtain $T_{\text{gas}} = 3.26\text{K}$ at $z = 17$, required for the EDGES signal. For the large magnetic field, saturation in the DM-baryon cross-section occurs at smaller values of the DM mass

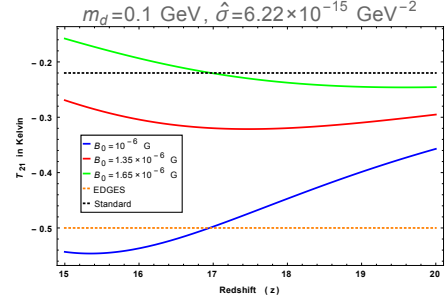


FIG. 3: Brightness temperature vs red shift for different magnetic fields when $m_d = 0.1\text{ GeV}$ and $\hat{\sigma} = 10^{-15}\text{ GeV}^{-2}$. The dotted black (orange) color represent standard ΛCDM (EDGES) predictions for the global T_{21} signal and the green, red and blue solid lines correspond to $B_0 = 10^{-6}, 1.35 \times 10^{-6}$ and $1.65 \times 10^{-6}\text{G}$ respectively.

because low mass favours less heating compared to the high mass due to the drag term.

Effect of strong magnetic field on brightness temperature

We have discussed above that, as we increase the strength of the magnetic field, for a fix DM mass and interaction cross section, temperature of the gas increases. The differential brightness temperature T_{21} during $15 \leq z \leq 20$ can be obtained by taking $T_S = T_{\text{gas}}$ in Eq. (3) for different magnetic field. For $B_0 = 10^{-6}\text{G}$, the brightness temperature for EDGES reported signal (i.e. -0.5K) can be explained when $m_d = 0.1\text{ GeV}$ and $\hat{\sigma} = 6.22 \times 10^{-15}\text{ GeV}^{-2}$. As shown in Fig.(3), brightness temperature is suppressed by the increase of the strength of the magnetic field and it can even erase the standard 21 cm signal when the magnetic field strength increases above $1.65 \times 10^{-6}\text{G}$. This sets the upper limit on the strength of the magnetic field for $m_d = 0.1\text{ GeV}$ and $\hat{\sigma} = 6.22 \times 10^{-15}\text{ GeV}^{-2}$.

VI. CONCLUSION

In the present work, we have studied the evolution of the baryon and the DM temperature along with the 21-cm brightness temperature with red-shift in the presence of the heating from magnetic fields and drag between the two fluids i.e. baryon and DM. We have studied the effect of magnetic energy dissipation via ambipolar diffusion and turbulent decay on baryon-DM interaction during the cosmic dawn era. The magnetic-energy converted to the thermal energy, heat up both

the gas and dark matter. This is an extra heating effect in addition to the drag heating. The drag term also heats up the DM and the baryon due to the relative motion of the two fluids. However, we have found that the magnetic heating is more in favour of the baryons compared to the DM. In order to explain the observed anomaly in the 21-cm signal by the EDGES, a large baryon-DM scattering cross-section is required to balance the magnetic heating effect. An earlier saturation occurs in baryon-DM cross-section with respect to the DM mass in the presence of the high magnetic fields.

-
- [1] C. J. Hogan and M. J. Rees, *MNRAS* **188**, 791 (1979).
- [2] D. Scott and M. J. Rees, *MNRAS* **247**, 510 (1990).
- [3] A. Fialkov, R. Barkana, and E. Visbal, *Nature* **506**, 197 (2014), arXiv:1402.0940 [astro-ph.CO].
- [4] J. D. Bowman, A. E. E. Rogers, R. A. Monsalve, T. J. Mozdzen, and N. Mahesh, *Nature* **555**, 67 (2018), arXiv:1810.05912 [astro-ph.CO].
- [5] R. Barkana, N. J. Outmezguine, D. Redigolo, and T. Volansky, *Phys. Rev. D* **98**, 103005 (2018).
- [6] R. Barkana, *Nature* **555**, 71 (2018), arXiv:1803.06698 [astro-ph.CO].
- [7] H. Tashiro, K. Kadota, and J. Silk, *Phys. Rev. D* **90**, 083522 (2014), arXiv:1408.2571 [astro-ph.CO].
- [8] C. Dvorkin, K. Blum, and M. Kamionkowski, *Phys. Rev. D* **89**, 023519 (2014), arXiv:1311.2937 [astro-ph.CO].
- [9] A. Berlin, D. Hooper, G. Krnjaic, and S. D. McDermott, *Phys. Rev. Lett.* **121**, 011102 (2018), arXiv:1803.02804 [hep-ph].
- [10] C. Creque-Sarbinowski, L. Ji, E. D. Kovetz, and M. Kamionkowski, (2019), arXiv:1903.09154 [astro-ph.CO].
- [11] T. Moroi, K. Nakayama, and Y. Tang, *Phys. Lett. B* **783**, 301 (2018), arXiv:1804.10378 [hep-ph].
- [12] G. D'Amico, P. Panci, and A. Strumia, *Phys. Rev. Lett.* **121**, 011103 (2018), arXiv:1803.03629 [astro-ph.CO].
- [13] A. Mitridate and A. Podo, *JCAP* **1805**, 069 (2018), arXiv:1803.11169 [hep-ph].
- [14] H. Liu and T. R. Slatyer, *Phys. Rev. D* **98**, 023501 (2018), arXiv:1803.09739 [astro-ph.CO].
- [15] J. R. Bhatt, A. K. Mishra, and A. C. Nayak, (2019), arXiv:1901.08451 [astro-ph.CO].
- [16] M. S. Turner and L. M. Widrow, *Phys. Rev. D* **37**, 2743 (1988).
- [17] R. Sharma, K. Subramanian, and T. R. Seshadri, *Phys. Rev. D* **97**, 083503 (2018), arXiv:1802.04847 [astro-ph.CO].
- [18] J. R. Bhatt and A. K. Pandey, *Phys. Rev. D* **94**, 043536 (2016), arXiv:1503.01878 [astro-ph.CO].
- [19] S. Anand, J. R. Bhatt, and A. K. Pandey, *JCAP* **1707**, 051 (2017), arXiv:1705.03683 [astro-ph.CO].
- [20] K. Subramanian, *Rept. Prog. Phys.* **79**, 076901 (2016), arXiv:1504.02311 [astro-ph.CO].
- [21] P. Kronberg, *Reports on Progress in Physics* **57**, 325 (1994).
- [22] A. Neronov and I. Vovk, *Science* **328**, 73 (2010), arXiv:1006.3504 [astro-ph.HE].
- [23] P. Trivedi, T. R. Seshadri, and K. Subramanian, *Phys. Rev. Lett.* **108**, 231301 (2012).
- [24] P. Trivedi, K. Subramanian, and T. R. Seshadri, *Phys. Rev. D* **89**, 043523 (2014), arXiv:1312.5308 [astro-ph.CO].
- [25] P. A. R. Ade *et al.* (Planck), *Astron. Astrophys.* **594**, A19 (2016), arXiv:1502.01594 [astro-ph.CO].
- [26] B. Cheng, A. V. Olinto, D. N. Schramm, and J. W. Truran, *Phys. Rev. D* **54**, 4714 (1996).
- [27] D. Grasso and H. R. Rubinstein, *Phys. Rept.* **348**, 163 (2001), arXiv:astro-ph/0009061 [astro-ph].
- [28] J. J. Matese and R. F. O'Connell, *Phys. Rev.* **180**, 1289 (1969).
- [29] G. GREENSTEIN, *Nature* **223**, 938 (1969).
- [30] H. Tashiro and N. Sugiyama, *Mon. Not. Roy. Astron. Soc.* **368**, 965 (2006), arXiv:astro-ph/0512626 [astro-ph].
- [31] S. K. Sethi and K. Subramanian, *Mon. Not. Roy. Astron. Soc.* **356**, 778 (2005), arXiv:astro-ph/0405413 [astro-ph].
- [32] J. R. Pritchard and A. Loeb, *Rept. Prog. Phys.* **75**, 086901 (2012), arXiv:1109.6012 [astro-ph.CO].
- [33] S. A. Wouthuysen, *aj* **57**, 31 (1952).
- [34] G. B. Field, *apj* **129**, 536 (1959).
- [35] K. Jedamzik, V. c. v. Katalinić, and A. V. Olinto, *Phys. Rev. D* **57**, 3264 (1998).
- [36] K. Subramanian and J. D. Barrow, *Phys. Rev. D* **58**, 083502 (1998), arXiv:astro-ph/9712083 [astro-ph].
- [37] C. J. Hogan, *Phys. Rev. Lett.* **51**, 1488 (1983).
- [38] R. Durrer and C. Caprini, *JCAP* **0311**, 010 (2003), arXiv:astro-ph/0305059 [astro-ph].
- [39] H. Tashiro and N. Sugiyama, *Mon. Not. Roy. Astron. Soc.* **372**, 1060 (2006), arXiv:astro-ph/0607169 [astro-ph].
- [40] N. Aghanim *et al.* (Planck), (2018), arXiv:1807.06209 [astro-ph.CO].
- [41] T. G. Cowling, *MNRAS* **116**, 114 (1956).
- [42] F. H. Shu, *The physics of astrophysics. Volume II: Gas dynamics.*, University Science Books, Mill Valley, CA (USA), ISBN 0-935702-65-2 (1992).
- [43] H. Shang, A. E. Glassgold, F. H. Shu, and S. Lizano, *Astrophys. J.* **564**, 853 (2002), arXiv:astro-ph/0110539 [astro-ph].
- [44] B. T. Draine, *APJ* **241**, 1021 (1980).
- [45] D. R. G. Schleicher, R. Banerjee, and R. S. Klessner, *Phys. Rev. D* **78**, 083005 (2008), arXiv:0807.3802 [astro-ph].
- [46] D. R. G. Schleicher, R. Banerjee, and R. S. Klessner, *Astrophys. J.* **692**, 236 (2009), arXiv:0808.1461 [astro-ph].
- [47] J. B. Muñoz, E. D. Kovetz, and Y. Ali-Haïmoud, *Phys. Rev. D* **92**, 083528 (2015).
- [48] Y. Ali-Haïmoud and C. M. Hirata, *Phys. Rev. D* **83**, 043513 (2011), arXiv:1011.3758 [astro-ph.CO].
- [49] T. Minoda, H. Tashiro, and T. Takahashi, (2018), arXiv:1812.00730 [astro-ph.CO].